

1
2
3
4
5
6
7
8
9
10
11
12
13
14
15
16
17
18
19
20

Matilda v1.0: An R package for probabilistic climate projections using a reduced complexity climate model

Matilda: An R framework for probabilistic climate analysis

Joseph K Brown*, Leeya Pressburger, Abigail Snyder, Kalyn Dorheim, Steven J Smith, Claudia Tebaldi, and Ben Bond-Lamberty

Joint Global Change Research Institute, Pacific Northwest National Laboratory, 5825 University Research Ct. #3500, College Park, MD 20740 USA

*Corresponding author
Email: joseph.brown@pnnl.gov

21 Abstract

22 A primary advantage to using reduced complexity climate models (RCMs) has been their ability
23 to quickly conduct probabilistic climate projections, a key component of uncertainty
24 quantification in many impact studies and multisector systems. Providing frameworks for such
25 analyses has been a target of several RCMs used in studies of the future co-evolution of the
26 human and Earth systems. In this paper, we present `Matilda`, an open-science R software
27 package that facilitates probabilistic climate projection analysis, implemented here using the
28 Hector simple climate model in a seamless and easily applied framework. The primary goal of
29 `Matilda` is to provide the user with a turn-key method to build parameter sets from literature-
30 based prior distributions, run Hector iteratively to produce perturbed parameter ensembles
31 (PPEs), weight ensembles for realism against observed historical climate data, and compute
32 probabilistic projections for different climate variables. This workflow gives the user the ability
33 to explore viable parameter space and propagate uncertainty to model ensembles with just a
34 few lines of code. The package provides significant freedom to select different scoring criteria
35 and algorithms to weight ensemble members, as well as the flexibility to implement custom
36 criteria. Additionally, the architecture of the package simplifies the process of building and
37 analyzing PPEs without requiring significant programming expertise, to accommodate diverse
38 use cases. We present a case study that provides illustrative results of a probabilistic analysis of
39 mean global surface temperature as an example of the software application.
40

41 1 Introduction

42 The human-Earth system is fundamentally integrated with impacts and feedbacks tightly
43 interconnecting outcomes across human decisions and the broader environment. Human
44 decisions regarding land use, water use, and energy consumption affect the broader Earth
45 system, which can subsequently drive future human decisions [\[1,2\]](#). Multisectoral models are
46 those that include representations of energy, water, land, socioeconomic, and climate sectors
47 in an integrated framework. The Global Change Analysis Model (GCAM), and similar
48 multisectoral models can be used to explore future scenarios with different water, energy, land
49 use, and socioeconomic outcomes that interact with the Earth system. Representative
50 Concentration Pathways (RCPs), for example, provide scenarios that reach varying magnitudes
51 of radiative forcing by the end of the century based on changing GHG emissions and land use
52 [\[1–3\]](#). Shared Socio-economic Pathways (SSPs) provide scenarios driven by plausible changes in
53 global developments including population and economic growth, fossil fuel dependency, and
54 costs of environmental degradation [\[3,4\]](#). The development of an SSP-RCP framework
55 (hereafter, SSPs) combines the climate and societal futures of SSPs and RCPs [\[3,5\]](#). These
56 scenarios can be used in Earth system models (ESMs) to explore future climate outcomes given
57 different possible emissions scenarios. However, the breadth at which ESMs can investigate the
58 climate system comes at a significant computational expense.
59

60 Reduced complexity climate models (RCMs) play a significant role in quickly assessing how key
61 climate variables may look in the future by applying probabilistic projections, which are made
62 possible because of their simplified computational complexity [6–11]. By representing only the
63 most critical Earth system processes with reduced resolution in temporal and spatial
64 dimensions, RCMs are a useful alternative to more powerful but much slower ESMs in many
65 cases [9,12]. The computational efficiency of RCMs makes them an ideal tool for constructing
66 perturbed parameter ensemble (PPE) simulations, which are RCM ensembles built by running
67 the model iteratively with different parameter sets [7,13,14]. This ability enables effective
68 sampling of the parameter space, propagation of parameter uncertainty to RCM ensembles,
69 and provides a framework for probabilistic projection quantification [7–9,15,16].

70
71 The capacity for RCMs to conduct probabilistic projections with PPEs is critical, but few RCMs
72 have an easy-to-use and open-source workflow for this capability. In Phase 2 of the Reduced
73 Complexity Model Intercomparison Project (RCMIP), Nicholls et al. [17] highlight the use of
74 extant RCMs to perform probabilistic analyses to inform Earth system knowledge by creating
75 PPEs. Among the RCMIP models investigated; MAGICC, FaIR, and Hector are some of the most
76 relevant, with MAGICC and FaIR used in previous reports by the Intergovernmental Panel on
77 Climate Change (IPCC) [12]. While both models are extensive and widely used for probabilistic
78 projections [18–20], they have some drawbacks. For example, while FaIR demonstrates skillful
79 outputs in RCMIP evaluations [17], it lacks a turnkey mechanism for computing probabilistic
80 distributions of climate variables [7,14]. This places a significant programming responsibility on
81 the user. Hector has similarly lacked a seamless method for probabilistic projections. MAGICC
82 is also one of the best-performing RCMs in RCMIP and takes advantage of a rigorous statistical
83 approach [10,21]. However, while it aims to shift to open-source, it is currently a closed-source
84 model. To use MAGICC to the fullest capability of the model, users must contact model
85 developers for access to the software package and probabilistic distribution.

86
87 We address some of these drawbacks in our development of the R package Matilda. Matilda
88 is an open-science framework that provides a simplified method for conducting probabilistic
89 climate projections without imposing a significant programming burden on the user. Our
90 method generates parameter sets from Monte Carlo estimation of prior distributions from the
91 literature. It then builds PPEs, weights them for realism against observed data, and computes
92 probabilistic climate projections. While Matilda is flexible enough to operate with many
93 RCMs, it was designed explicitly for seamless integration with Hector.

94
95 Hector is an open-source, object-oriented simple climate carbon-cycle model capable of
96 emulating more complex ESMs and is executed in C++ [6,9,11]. It takes advantage of the
97 computational benefits described above by operating on a global spatial scale and annual time
98 step. The model functions by converting user-specified emissions to atmospheric
99 concentrations which are used to calculate radiative forcing [6,9]. Hector then uses total
100 radiative forcing to derive global temperature change and other climate variables [9,11].
101 Despite its reduced complexity, Hector provides a good representation of CMIP6 outputs for
102 major climate variables across SSP scenarios [22]. In addition to operating as a stand-alone

103 carbon-climate model, Hector is also used as the default climate module for GCAM [6]. Hector
104 can also be run as an R package and through a web-accessible interface, making it
105 accommodating to a larger user base [22–24]. Hector’s design and performance make it an
106 excellent candidate for developing a user-friendly probabilistic climate projection tool in R.
107 Pressburger et al. [13] show the benefits of applying such a framework to account for
108 uncertainty of model parameters when assessing near- and long-term sources of atmospheric
109 CO₂. With Matilda, users will be able to easily use Hector to conduct probabilistic climate
110 projection analyses without the burden of complex coding requirements. Matilda thus
111 provides seamless integration with the Hector reduced complexity climate model.

112
113 The objectives of this paper are twofold: 1) we introduce the Matilda R package that provides
114 a simple framework for conducting probabilistic climate projection analyses using the Hector
115 simple climate model and 2) we showcase the package functionality with a case study that
116 provides illustrative results but is not meant to be a comprehensive probabilistic analysis. We
117 conclude with a list of future developments that can improve the long-term utility of Matilda.

118 2 Software Description

119 Here we introduce the software functions and basic workflow of the package (Fig. 1). We use
120 applied examples to show package functionality by assessing climate change projections from
121 the SSP 2-4.5 emissions scenario (i.e., middle of the road SSP with the year 2100 radiative
122 forcing level of 4.5 W/m²), providing step-by-step code and explaining the significance of each
123 function.

124
125 **Fig 1. Matilda workflow.** Diagram detailing the Matilda workflow to compute probabilistic
126 projections. Dotted lines indicate opportunities for the user to define their own program
127 specification. The dashed line in step 3 indicates the ability of the user to evaluate ensemble
128 members repeatedly with different scoring criterion.

129 2.1 Installing the Software

130 The Matilda software is available on GitHub. To install from our GitHub repository:

131
132 1)

```
library(remotes)  
install_github("jgcri/matilda")
```

133
134 Once installed, the package is loaded as with any other R package:

135
136 2)

```
library(matilda)
```

137

138 Matilda functions are fully integrated with Hector’s R interface, and therefore when
139 Matilda is installed and loaded, the hector package (<https://jgcri.github.io/hector/>) is also
140 loaded. Matilda requires the use of Hector V3 or newer [22].

141 2.2 Software Documentation

142 Full descriptions of package functions can be accessed in the package’s help documentation.
143 Furthermore, detailed documentation and vignettes are available from our GitHub repository
144 (github.com/jgcri/matilda).

145 2.3 Configuring a Model Core

146 An analysis in Matilda begins by setting up a Hector model instance, termed a “core”. A Hector
147 core is an object that contains information about model inputs, current state, and outputs for a
148 specific Hector run. The information contained in an initiated core comes from an INI file
149 holding metadata, emissions scenarios, and model parameters needed to run Hector.

150
151 We call `newcore()` (a hector function) to initiate a core containing information to conduct
152 model runs using the SSP 2-4.5 emission scenario:

```
153  
154 3)  
ini_file <- system.file("input/hector_ssp245.ini", package = "hector")  
core_ssp245 <- newcore(ini_file, name = "SSP_245")
```

155

156 2.4 Parameter Estimation and Establishing Parameter Sets

157 The basis of running Hector in a probabilistic setup relies on establishing a set of parameter
158 configurations that are used to run the model iteratively. Matilda uses parameter information
159 gathered from the literature to inform prior distributions (Table 1). To build parameter sets, we
160 draw parameter values from their prior distributions using Monte Carlo sampling. Each
161 parameter is sampled independently from its marginal prior distributions defined using mean
162 and standard deviation estimates as in:

$$163 \theta_i \sim N(\mu, \sigma) \quad (1)$$

164
165 where θ_i is a given Hector parameter and $N(\mu, \sigma)$ is the normal distribution of parameter θ_i
166 using hyperparameters μ (mean) and σ (standard deviation). Some parameters have marginal
167 distributions best represented using lognormal distribution, in such cases, $N(\mu, \sigma)$ is substituted
168 by $\text{log}N(\mu, \sigma)$ (Table 1). Using informed prior marginal distributions from the literature as a
169 starting point for building perturbed parameter sets enables the exploration of a range of
170 possible parameter values from viable parameter space built on existing knowledge [13,25].
171 Parameter draws are combined into parameter sets for Hector using a uniform multivariate
172

173 distribution. This parameter estimation process ultimately establishes parameter sets that
174 account for parameter uncertainty and can be used to build an ensemble of model runs. In
175 other words, we use prior information about individual parameters to build parameter sets, but
176 we do not know which sets will result in the most skilled model results before considering
177 observed data.
178

Table 1. Hector parameters used in Matilda. Hector parameters used to generate parameter sets in this work. The distributions are indicated as mean \pm standard deviation. References from where distributions are derived are included.

Parameter	Description	Units	Distribution	Reference of uncertainty
α	Aerosol forcing scaling factor	Unitless	1.0 ± 0.23 (Normal)	Smith et al (2020) (25)
β	CO ₂ fertilization factor	Unitless	0.55 ± 0.10 (Normal)	Jones et al (2013) (26)
ECS	Equilibrium Climate Sensitivity	°C	3.0 ± 0.65 (Lognormal)	Sherwood et al (2020) (27)
K_{eff}	Ocean heat diffusivity	cm ² s ⁻¹	1.16 ± 0.118 (Normal)	Vega-Westhoff et al (2019) (28)
NPP ₀	Pre-industrial net primary productivity	Pg C yr ⁻¹	56.2 ± 14.3 (Normal)	Ito (2011) (29)
Q ₁₀	Temperature sensitivity of heterotrophic respiration	Unitless	2.2 ± 1.0 (Lognormal)	Davidson and Janssens (2006) (30)

179
180 In `Matilda`, we build parameter sets by calling `generate_params()`. Parameter distributions
181 are independent of the SSP scenario, however to run this function the user must still provide an
182 established Hector core. Additionally, the user must specify the number of parameter sets
183 desired (`draws`). Using `generate_params()` will produce randomized draws each time it is run.
184 Therefore, the user should either save the resulting data frame or use `set.seed()` if replication
185 of parameter sets is critical to the analysis. In this example we use our previously established
186 core to produce a set of 25 parameter configurations and display a subset of samples from the
187 result:

188
189

```
4)
param_sets <- generate_params(core = core_ssp245, draws = 25)
print(param_sets)
```

190

```
##      BETA      Q10_RH  NPP_FLUX0  AERO_SCALE  DIFFUSIVITY      ECS
## 1 0.5429609 1.7033771 50.47088 1.2697224 1.070107 2.410262
## 2 0.5234430 1.4867288 51.41584 0.6596398 1.209486 3.092423
## 3 0.4225671 1.3724196 75.76174 0.9010108 1.037287 2.335147
## 4 0.4857051 1.9163999 86.77007 0.7581231 1.243966 2.712076
```

191
192 Parameters can be easily added or omitted from the new parameter set data frame. For
193 example, to run the model with a subset of parameters, undesired columns can be omitted
194 from the data frame. This will result in a data frame that only contains parameter distributions
195 that the user wishes to perturb. Similarly, the user can characterize additional parameter
196 distributions and add them as new columns to the data frame, as long as the parameter is
197 described in Hector.

198
199 Once established, the parameter sets are used as inputs for independent Hector model runs.
200 Thus, each model run represents a multivariate parameter combination as follows:

$$201 \\ 202 m_i = (\theta_{1_i}, \theta_{2_i}, \theta_{3_i}, \dots, \theta_{n_i}) \quad (2)$$

203
204 where m_i is an individual ensemble member and $\theta_{\{1-n\}_i}$ are parameters sampled to build an
205 independent configuration. Using different parameter sets to run Hector allows us to build PPEs
206 and determine how different parameter combinations from a viable parameter space interact
207 to affect climate variable projections. This method effectively propagates parameter
208 uncertainty to model ensemble uncertainty, a process described as forward uncertainty
209 propagation [32].

210 2.5 Forward Uncertainty Propagation and Running the Model

211 We run Hector for each of the parameter sets by calling `iterate_model()`, which runs the
212 model for each parameter set and combines the results into a data frame object representing
213 the new PPE. To run `iterate_model()`, the same core object is used as in previous steps and
214 we also must supply the object where parameter sets are stored:

```
215 5)  
216 results <- iterate_model(core = core_ssp245, params = param_sets)  
  
print(results)
```

```
217  
##      scenario year      variable      value      units run_number  
## 1 Unnamed Hector core 1745 CO2_concentration 277.1500 ppmv CO2      1  
## 2 Unnamed Hector core 1746 CO2_concentration 277.1886 ppmv CO2      1  
## 3 Unnamed Hector core 1747 CO2_concentration 277.2234 ppmv CO2      1  
## 4 Unnamed Hector core 1748 CO2_concentration 277.2558 ppmv CO2      1
```

218

219 The resulting data frame returns 25 separate runs, as indicated by the `run_number` column; in
220 this case, the total number of rows is 55600 (25 runs \times 4 output variables \times 556 years). Each run
221 includes values for the major climate variables of a Hector default output (CO₂ concentration,
222 total radiative forcing, CO₂ forcing, and global mean air temperature) for the years 1745-2300
223 (the time range defined by the SSP INI file we chose above).

224
225 While a core object and a data frame of parameter sets are the only required arguments to run
226 `iterate_model()`, additional arguments can be supplied to reduce the variables and year
227 range returned for each run using `save_vars` and `save_years`, respectively. This reduces the
228 size of the data stored in memory, which may be important when running the model to build
229 large ensembles (e.g., 15,000 as in [13]). Any output variable from Hector can be returned using
230 `save_vars()` for any year range subset from 1745-2300. In the following example, we supply
231 these arguments to return values only for CO₂ concentration and global mean air temperature
232 for the year range 1745-2100:

```
233  
234 6)  
    results<- iterate_model(core = core_ssp245, params = param_sets, save_vars  
    = c("CO2_concentration", "global_tas"), save_years = 1745:2100)
```

235
236 The resulting data frame has only 17800 rows, a 68% savings over the full example above.

237 2.6 Model Evaluation Approach and Scoring Model Runs

238
239 Evaluating ensemble members is important in climate model assessment because it allows for a
240 more accurate representation of the true underlying system by accounting for uncertainties
241 propagated from parameter sets. The concept of weighting ensemble members is intuitive;
242 members that are skilled and agree well with the historical record should receive a higher
243 weight than members that do not largely replicate what we know to be a realistic climatic
244 projection [8]. By assigning weights to ensemble members, based on their performance against
245 observed data, more reliable projections can be made for future climate scenarios as
246 parameter uncertainty is propagated to model forecasts. Ensemble members closely aligned
247 with historical climate data will contribute more information to our probabilistic projections
248 than members with outputs deviating significantly from the historical record. In parallel, we can
249 use forward uncertainty propagation to better understand what parameter sets interact with
250 Hector in a way that yields the most realistic result. This can then be used to update prior
251 parameter distributions (although we do not do so here).

252
253 Scoring PPE members in Matilda is conducted using `score_runs()` which requires (1) a
254 results data frame, (2) a scoring criterion, and (3) a scoring function/algorithm. The results data
255 frame typically comes from calling `iterate_model()`, as above.

256

257 Scoring criteria define information used to compare ensemble members against observational
258 data. A scoring criterion can be built by the user by calling `new_criterion()` and simply
259 requires the climate variable to be used in the comparison, the years of comparison, and
260 observed data values for the years specified. For example, a new criterion can be created based
261 on global mean air temperature from a dataset containing observed warming values from 1990-
262 2023:

263
264 7)

```
temp_data <- read.csv("example_temperature_data.csv")
```

```
head(temp_data)
```

265

```
##   year anomaly_C  
## 1 1990 0.3605625  
## 2 1991 0.3388965  
## 3 1992 0.1248968  
## 4 1993 0.1656585  
## 5 1994 0.2335498  
## 6 1995 0.3768662
```

266

```
user_temp_criterion <- new_criterion(var = "gmst", years = temp_data$year,  
obs_values = temp_data$anomaly_C)
```

```
print(user_temp_criterion)
```

267

```
## Criterion for screening Hector: gmst 1990 to 2023
```

268

269 This defines a custom criterion: a time series of 34 (1990-2023) values that will be compared
270 against Hector's "gmst" (global mean surface temperature anomaly) output variable.

271

272 The `Matilda` package has internally available scoring criteria for easy use, including
273 `criterion_co2_obs()` and `criterion_gmst_obs()`. Data contained in
274 `criterion_co2_obs()` is pulled from the Mauna Loa record of observed annual mean
275 atmospheric CO₂ concentration (32), while `criterion_gmst_obs()` uses observed annual
276 mean global surface temperature anomaly data retrieved from the HadCRUT5 data set (33).

277

278 Scoring functions in `Matilda` apply different mathematical algorithms to compute model
279 weights based on the results and scoring criterion. We provide multiple mechanisms to weight
280 model outputs against observations, and users can define their own custom functions as well.
281 There are currently two internally available scoring functions called `score_bayesian()` and
282 `score_ramp()`, that differ in functionality and computational complexity.

283 2.6.1 Scoring Function: `score_bayesian()`

284 Bayesian probability theory provides a rigorous framework combining prior information,
285 observational data, and model simulations to achieve analytical goals related to parameter
286 estimation, model evaluation, and uncertainty quantification [35,36]. Here, we use Bayesian
287 inference to assess PPE members and assign weights according to the probability of ensemble
288 member m_i conditional upon observed data \mathbf{Y} . This is described as the posterior probability
289 and, consistent with Bayes' theorem, is proportional to the product of a chosen likelihood
290 function of m_i given observed data and prior information of m_i (prior probability) [37]. We can
291 express this in equation form as:

$$292 \quad P(m_i|Y) \propto L(m_i|Y) \times P(m_i) \quad (3)$$

293
294 where $P(m_i|\mathbf{Y})$ is the posterior probability of m_i conditional upon observed data \mathbf{Y} , $L(m_i|\mathbf{Y})$ is
295 the chosen likelihood function, and $P(m_i)$ is the prior information of ensemble member m_i .

296
297 As demonstrated in Eq. 3, posterior probabilities (i.e., model weights) are dependent on prior
298 knowledge about ensemble member m_i and a likelihood function that quantifies the agreement
299 between ensemble member m_i and observed data \mathbf{Y} . Here, we base our likelihood function on
300 root-mean-square error (RMSE) which is commonly used as a statistical evaluation of model
301 performance in climate research and is optimal under the assumption that errors are normally
302 distributed [38,39]. For a given time series of observed data $\mathbf{Y}_{(t)}$ (i.e., scoring criteria) and a
303 corresponding time series of each ensemble member $m_{i(t)}$, RMSE is a quantification of the
304 averaged difference between the observed and modeled data and is calculated using the
305 following formula:

$$306 \quad RMSE_i = \sqrt{\frac{1}{N} \sum_{t=1}^N (\mathbf{Y}_t - m_{i(t)})^2} \quad (4)$$

307
308 where $RMSE_i$ is an independent RMSE value representing how well PPE member i agrees with
309 observations and N represents the total number of data points in the time series. We further
310 use these $RMSE_i$ values in our chosen likelihood function. Assuming a normal distribution, our
311 proportional likelihood can be calculated as:

$$312 \quad L(m_i|Y) = e^{-\frac{(RMSE_i)^2}{2\sigma^2}} \quad (5)$$

313
314 In this equation, a decay relationship exists between $RMSE_i$ and $L(m_i|\mathbf{Y})$, indicating a gradual
315 decrease in $L(m_i|\mathbf{Y})$ as $RMSE_i$ increases. In other words, the likelihood of an ensemble member
316 decreases as the disagreement with observations increases. The value of σ in Eq. 5 plays a
317 crucial role in controlling the rate of likelihood decay by defining the unit of acceptable variance
318 in the data. The relationship is explained in detail below and can be visualized in Fig 2.

322

323 As described in Section 2.4, we enforce an equally distributed prior $P(m_i)$ across all ensemble
324 members because although we use prior information about individual parameters of Hector to
325 build parameter sets, we do not know which sets will result in the most skilled model results
326 before considering observed data. Taking all this information together, weights are estimated in
327 `score_runs()` as normalized posterior probabilities of each ensemble member, taking into
328 account both agreement with observed data and prior beliefs about ensemble members using
329 the following formula:

$$\omega_i = \frac{L(m_i|Y) \times P(m_i)}{\sum_{i=1}^N (L(m_i|Y) \times P(m_i))} \quad (6)$$

332
333 where ω_i is a weight assigned to each ensemble member.

334
335 We provide an example of using `score_bayesian()` as the scoring function when calling
336 `score_runs()`. For this example, we use the result produced in code block 5, and assess the
337 agreement between ensemble members and observed data with the `criterion_co2_obs()`
338 scoring criterion:

```
339  
340 8)  
scored_hector_runs <- score_runs(results, criterion_co2_obs(),  
score_bayesian, sigma = 2)  
  
print(scored_hector_runs)
```

```
341  
##      weights  run_number  
## 1 0.093578592         1  
## 2 0.005328194         2  
## 3 0.138975159         3  
## 4 0.008768552         4  
## 5 0.040364027         5
```

342
343 The resulting data frame returns 25 weights assigned for each Hector run (indicated by
344 `run_number`). Weights for each ensemble member will be nonzero positive values that sum to
345 1. Weights closer to 1 represent ensemble members in strong agreement with observed data
346 and weights closer to 0 correspond to members that are not in strong agreement with observed
347 data. It is important to note that weights are asymptotic and thus no one ensemble member
348 can score exactly 1 or reach a value of exactly 0 due to the normalization process.

349
350 The `sigma` value in code block 8 is a parameter that sets the decay rate determining how
351 quickly the likelihood values decrease as RMSE values increase. Because `sigma` represents the
352 unit of acceptable deviation, a lower `sigma` value leads to a faster decay rate, meaning that the
353 likelihood decreases more rapidly with increasing RMSE values. Conversely, a higher `sigma`
354 reduces the decay rate, and ensemble member likelihood decreases more slowly with respect
355 to increasing RMSE values. This results in more weight being assigned to ensemble members

356 that have a lower likelihood. In Figure 2, we show how different `sigma` values lead to different
357 decay rates, meaning that weights are distributed differently depending on `sigma`. In effect,
358 this determines how severely an ensemble member is penalized as it departs from a criterion.
359

360 **Fig 2. Decay rates from varying sigma values.** Root mean square error (RMSE) plotted against
361 likelihood, conditional upon observed data. Different colors indicate decay rates for different
362 `sigma` values in `score_bayesian()`. Setting higher values to `sigma` decreases the deviation
363 penalty applied to ensemble members.
364

365 This parameter thus gives users the ability to govern the sensitivity of the likelihood decay as
366 RMSE values increase. By adjusting the `sigma` value, the user has control over the weight
367 assigned to different ensemble members based on their RMSE values. Setting a lower `sigma`
368 value will result in more weight placed on ensemble members with low RMSE values. In
369 comparison, a higher `sigma` value will give relatively more weight to ensemble members with
370 higher RMSE values. We use the standard deviation of the observed data as the default
371 quantification of `sigma`, which results in a relatively gradual tapering of the likelihood as RMSE
372 increases. We provide options in `score_bayesian()` to set a value to `sigma` directly or to
373 weight ensemble members within easily defined units of acceptable deviation from observed
374 data.
375

376 We note that users should make adjustments to `sigma` that are in line with the context and
377 evaluation purpose specific to their analytical goals. The case study at the end of this paper
378 provides an example of assessing ensemble member weights for different acceptable deviation
379 limits.

380 2.6.2 Scoring Function: `score_ramp()`

381 The `score_ramp()` function is a simpler and more transparent scoring algorithm that computes
382 the absolute difference between ensemble members $m_i(t)$ and observed data $Y(t)$ at each time
383 step:

$$384 \quad D(t) = |Y(t) - m_i(t)| \quad (7)$$

385
386 Scores are then computed based on how far absolute differences $D(t)$ are from arbitrarily
387 selected minimum (w_1) and maximum (w_2) divergence values. For example, $D(t) \leq w_1$ indicates
388 small differences between modeled and observed data at time t and will result in a score of 1,
389 whereas $D(t) \geq w_2$ indicates significant divergence of modeled data from observed data and will
390 result in a score of 0 (Fig 3). In cases where $D(t)$ falls between w_1 and w_2 , scores are computed
391 using a linear function that decreases as $D(t)$ values get closer to w_2 and further from w_1 (Fig 3).
392
393

394 **Fig 3. Decay rate for `score_ramp()`.** Example of decay method for `score_ramp()` where $w_1 = 5$
395 and $w_2 = 10$. Ensemble members with an average deviation from observation < 5 will score 1
396 and ensemble members with an average deviation > 10 will score 0. Scores of ensemble

397 members with average deviation between w_1 and w_2 will decrease from 1 linearly as average
398 deviation approaches w_2 .

399

400 We can express this linear decay with the following formula:

401

$$402 \quad S(t) = \frac{(w_2 - D(t))}{(w_2 - w_1)} \quad (8)$$

403

404 where $S(t)$ is the score at time t . Once computed, scores are averaged across the entire time
405 series, resulting in a single score for each ensemble member. Scores for ensemble members are
406 normalized in `score_runs()` to assign a weight between 0-1 to skilled versus unskilled
407 members, where more skilled ensemble members will be weighted closer to 1 while less skilled
408 ensemble members will receive weights closer to 0. Similar to the normalization step above,
409 weights are estimated using the following formula:

410

$$411 \quad \omega_i = \frac{S_i(t)}{\sum_{i=1}^N (S_i(t))} \quad (9)$$

412

413 where ω_i is a weight assigned to each ensemble member from the normalized mean score of
414 each member $S_i(t)$.

415

416 Below we provide a code example using `score_ramp()` as the scoring function in a
417 `score_runs()` call. As in code block 8, we use the results produced in code block 5 and assess
418 the agreement between ensemble members and observed data with the
419 `criterion_co2_obs()` scoring criterion:

420

421 9)

```
scores <- score_runs(result, criterion_co2_obs(), score_ramp, w1=0, w2=10)
print(scores)
```

422

```
##      weights      run_number
## 1 1.044760e-02          1
## 2 7.575543e-10          2
## 3 6.271913e-02          3
## 4 8.717546e-21          4
## 5 6.774904e-13          5
```

423

424 Similar to scoring ensemble members with `score_bayesian()`, the resulting data frame
425 returns 25 weights assigned to each ensemble member (indicated by `run_number`).

426

427 Weighted ensemble members can be used to visualize a cone of uncertainty to help understand
428 error produced from known parameter combinations and/or parameter sampling distributions.
429 In Figure 4, we show all ensemble members weighted using our two scoring algorithms. The

430 ensemble shading visually demonstrates how `score_bayesian()`, with a default `sigma`,
431 distributes weights more evenly across likely ensemble members, whereas `score_ramp()`
432 assigns higher weights to ensemble members falling closer to the minimum divergence range of
433 w_1 (when $w_1 = 0$ and $w_2 = 10$ ppm).
434

435 **Fig 4. Weighted ensemble members using different scoring algorithms.** Perturbed parameter
436 ensemble (PPE) projections plotted for atmospheric CO₂ concentration from 1960-2100
437 weighted using the A) `score_ramp()` and B) `score_bayesian()` algorithms. Ensemble
438 member weights are indicated by color shading with the solid red line representing observed
439 atmospheric CO₂ concentrations from 1959-2021.
440

441 A time test on an analysis weighting 1000 ensemble members shows that the difference in
442 computation time between the two scoring algorithms is negligible, with both functions
443 computing weights for $N = 1000$ runs in a fraction of a second. Despite the similarities between
444 the two scoring algorithms, the differences in approach and customization options can lead to
445 variations in the behavior and performance of each method (Fig 4). It is therefore important to
446 consider the specific goals of an analysis and characteristics of the data when selecting which
447 scoring algorithm to use. Ultimately, differences in weights produced by the different scoring
448 algorithms will impact the probabilistic projections of resulting variables.

449 2.7 Defining and Calculating Metrics and Probabilities

450 Once the ensemble members are scored we can use them to compute informative metrics from
451 model projections. Calculating metrics from the final weighted PPE requires (1) a results data
452 frame and (2) a metric object, which must first be defined by the user.
453

454 Metric objects determine what data the user is most interested in extracting and summarizing
455 from the results data frame. For example, a metric object can identify information needed to
456 estimate global mean air temperature (`global_tas`) for the 20-year average used by the IPCC
457 to represent long-term temperature change (2081-2100). We complete this by calling the
458 function `new_metric()`:
459

460 10)

```
metric_lt <- new_metric(var = "global_tas", years = 2081:2100, op = mean)  
print(metric_lt)
```

461

```
## Probabilistic Hector Metric: mean global_tas 2081 to 2100
```

462

463 This defines a new custom metric object: obtain the mean global air temperature (`global_tas`)
464 for the years 2081-2100. The argument `op` in code block 10 describes an operation that can be
465 performed on the model data to compute a descriptive statistic for each member of the
466 ensemble. While we define a 20-year mean `global_tas` metric in this example, the user can also

467 easily compute the median, min, max, standard deviation, etc. for each ensemble member.
468 Additionally, users can specify a single year rather than quantifying statistics over a range of
469 years (e.g., 2100 vs. 2081-2100).

470
471 Once this metric is defined, we call `metric_calc()` to compute metric values for each
472 ensemble member using the results data frame:

```
473  
474 11)  
    values_metric_lt <- metric_calc(results, metric_lt)  
  
    print(values_metric_lt)
```

```
475  
  
##      run_number metric_result  
## 1           1      2.315857  
## 2           2      3.083498  
## 3           3      2.232456  
## 4           4      2.474680  
## 5           5      1.975036
```

476
477 The resulting data frame returns 25 separate metric values (indicated by the `metric_result`
478 column) representing the 2081-2100 mean warming of global air temperature.

479
480 When metrics of interest are calculated and weights are assigned to PPE members based on
481 agreement with historical record, we have the necessary information to address questions such
482 as, “*What is the probability that long-term mean temperature change will remain between 2.0-*
483 *3.5 °C relative to pre-industrial reference?*”

484
485 We approach such a question by calling `prob_calc()`, a function that sums PPE weights as they
486 are binned into metric ranges identified by the user. Running `prob_calc()` requires (1) a data
487 frame where metric values can be identified, (2) bins defined by the user, and (3) a data frame
488 where PPE weights can be identified. Here, we provide an example of `prob_calc()` usage:

```
489  
490 12)  
  
# Establishing metric ranges  
temp_range <- c(1.5, 2.0, 2.5, 3.0, 3.5, 4.0, Inf)  
  
# Producing probabilities  
prob_calc(metrics = values_metric_lt$metric_result,  
          bins = temp_range,  
          scores = scored_hector_runs$weights)
```

```
491  
  
##      bins      scores probability  
## 1 (1.5,2] 4.897565e-02 4.897565e-02  
## 2 (2,2.5] 3.802494e-01 3.802494e-01
```

```
## 3 (2.5,3] 5.707749e-01 5.707749e-01  
## 4 (3,3.5] 9.643701e-10 9.643701e-10  
## 5 (3.5,4] 1.122272e-08 1.122272e-08
```

492

493 In this example we use PPE weights computed using the `score_bayesian()` algorithm. The
494 `prob_calc()` result shows the total probability that long-term projections of mean warming
495 will fall within each of the temperature ranges defined by our bins (1.5-2 °C, 2-2.5 °C, 2.5-3 °C,
496 3-3.5 °C, 3.5-4 °C, and >4 °C) for the SSP scenario represented in our core object (SSP 2-4.5).
497 With the result above, for example, we can conclude that there is a 95% probability that the
498 long-term average global warming will remain between 2.0-3.0 °C relative to pre-industrial
499 reference.

500 3 Case Study: Probabilistic Temperature Projections 501 Across Four SSP Scenarios

502 Here, we present a case study to demonstrate the core utility of Matilda. We note that this case
503 study is meant only to show the utility of the package and is an illustrative example. It is not
504 meant to be presented as a full probabilistic analysis of temperature change from SSP
505 scenarios. In this case study we will use Hector with four SSP scenarios from CMIP6 (SSP1-1.9,
506 SSP1-2.6, SSP2-4.5, SSP3-7.0) [5] to compute mean temperature change over the long-term 20-
507 year average presented in IPCC AR6 [40]. We interpret our results similar to the IPCC, using
508 scaled likelihoods: very likely (90-100%), likely (66-100%), about as likely as not (33-66%),
509 unlikely (0-33%), and very unlikely (0-10%) [40]. This case study examines the probabilities of
510 long-term (2081-2100) global mean surface temperature change relative to a pre-industrial
511 reference in each of the four SSP scenarios.

512

513 After initiating cores for each of the four scenarios, we generate 1000 parameter sets using
514 `generate_params()`. For consistency, these 1000 parameter sets remain the same for each
515 scenario. We call `iterate_model()` to run Hector across all scenario cores using parameter
516 sets to propagate parameter uncertainty to PPE members. When running the models, we
517 extract the global mean surface temperature (`global_gmst`) for the years 1960-2100. Running
518 the model with 1000 parameter sets across four SSP scenarios takes ~100 minutes to run
519 serially on a single processor. Our resulting ensemble members are weighted by calling
520 `score_runs()`. We weighted ensemble members using observed mean annual global surface
521 temperature as a scoring criterion (`criterion_gmst_obs()`) with the Bayesian scoring
522 algorithm (`score_bayesian`).

523

524 Assessing different `sigma` values informs acceptable RMSE ranges for ensemble members and
525 weights them accordingly. For example, we show how weighting ensemble members using
526 `score_bayesian()` within one unit of the standard deviation of observed global mean surface
527 temperature (default `sigma`) places a higher likelihood on ensemble members with lower RMSE
528 values, while increasing the acceptable deviation limit to two units of the standard deviation of

529 the observed data decreases the penalty of ensemble members with relatively higher RMSE
530 values (Fig 5).

531
532 **Fig 5. Likelihood of ensemble members given different sigma values.** Likelihood of perturbed
533 parameter ensemble (PPE) members for an example emissions scenario based on root mean
534 square error (RMSE) using the `score_bayesian()` algorithm. Blue line shows the use of default
535 `sigma` value: The algorithm penalizes ensemble members as RMSE values deviate from
536 observed data by one unit of standard deviation. Red line shows the use of a customized `sigma`
537 value: Setting `sigma` to two units of standard deviation of observed values and thus assigns
538 weight to ensemble members falling within this acceptable deviation range. Black dots
539 represent individual ensemble members.

540
541 In this example analysis, we maintain `sigma` at its default value and then visualize PPE
542 members for each SSP scenario analyzed (Fig 6a). This provides some evidence of the range of
543 possible global mean surface temperature futures under each scenario. The most likely
544 outcomes are those that most accurately reflect historical global mean surface temperature
545 patterns (Fig 6a). To summarize the modeled data using our metric of interest (20-year mean of
546 global surface temperature for the years 2081-2100), we first establish our metric definition
547 using `new_metric()` and then call `metric_calc()` to compute metrics from our evaluated PPE.
548 For each SSP scenario, we compute probabilistic projections of long-term mean warming using
549 `prob_calc()` for 0.5 °C temperature bins for each SSP scenario (Fig 6b).

550
551 **Fig 6. Global mean surface temperature projections and warming probabilities across four**
552 **emissions scenarios.** A) 1000-member perturbed parameter ensemble (PPE) projecting global
553 mean surface temperature from 1950-2100 for each SSP scenario. Darker blue ensemble
554 members represent those members that best reflect historical temperature observations. B)
555 Stacked bars blocked by the probability of different temperature ranges for each SSP scenario.
556 Lower emissions scenarios (SSP1-1.9 and SSP1-2.6) have a higher probability of temperature
557 remaining below 2.0 °C than higher emissions scenarios (SSP2-4.5 and SSP3-7.0).

558
559 From this example, we can infer that when averaged over 2081-2100, the probability of
560 remaining below 2.0 °C warming decreases steadily as we transition from the low emissions
561 scenario (SSP1-1.9) to the higher emissions scenario (SSP3-7.0) (Fig. 6b). We can compute
562 approximate probabilities for different temperature ranges for the SSP scenarios by summing
563 probabilities in desired ranges. For example, in the low emission scenario SSP1-1.9, the
564 probability that warming will remain below 2.0 °C in our long-term warming projection is ~96%.
565 Alternatively, we can achieve precise probabilities by altering bin widths supplied to
566 `prob_calc()` to ranges that can be compared with IPCC results [40]. For example, in IPCC AR6
567 the SSP1-1.9 scenario is *very likely* (90-100%) to be warmer by 1.0 °C-1.8 °C relative to pre-
568 industrial reference, while the SSP3-7.0 scenario is *very likely* to be warmer by 2.8 °C-4.6 °C
569 [40]. We find similar results here, where SSP1-1.9 is *very likely* (97%) to be warmer by 1.0 °C-
570 2.0 °C and SSP3-7.0 is *very likely* (92%) to be warmer by 2.4 °C-4.8 °C relative to the pre-
571 industrial reference. For scenarios SSP1-2.6 and SSP2-4.5, the corresponding *very likely* ranges
572 in IPCC AR6 are 1.3-2.4 °C and 2.1-3.5 °C, respectively [40]. For these scenarios, we again find

573 *very likely* temperature ranges similar to what IPCC AR6 indicates, where SSP1-2.6 is *very likely*
574 (94%) to be warmer by 1.1 °C-2.6 °C and SSP2-4.5 is *very likely* (92%) to be warmer by 1.7 °C-3.8
575 °C relative to the pre-industrial reference.

576
577 The results from this example case study assume that models can be accurately evaluated using
578 a single scoring criterion (such as observed global mean surface temperature). However, it is
579 widely recognized that evaluating climate models often involves considering multiple lines of
580 evidence. For example, comprehensive model evaluation should involve assessing performance
581 across various observed climate variables (e.g., temperature and CO₂ concentrations and the
582 interactions that exist among those variables), as well as more complex models (i.e., ESMs). The
583 form of the scoring function is also non-univocal in most applications and motivates the
584 flexibility of Matilda in allowing different choices.

585 4 Conclusion

586 Using RCMs for probabilistic climate projections is critical for exploring uncertainty in the future
587 integrated human-Earth system [13,17–19]. The use of RCMs presents a viable approach to
588 tackle this challenge, as they possess the capability to simulate perturbed parameter ensembles
589 (PPEs) rapidly and can emulate the behavior of more complex ESMs [17] for some key large-
590 scale observable quantities. However, despite their proficiency, some challenges arise when
591 employing several RCMs for probabilistic climate projection analysis. These challenges include
592 closed-source designs and placing heavy programming responsibility on the user [7,10,14,21],
593 which can make both analysis and interpretation difficult.

594
595 Matilda is an open-source, turn-key, flexible framework that provides tools to complete
596 probabilistic climate projections using the Hector model. We show how this tool streamlines
597 probabilistic projection analysis and makes such analytical approaches more accessible to the
598 large community of R users, with seamless integration with Hector. By expanding the ways
599 Hector can be used, Matilda can help address questions of climate uncertainty under different
600 emissions scenarios and pursue other probabilistic analyses. We hope that Matilda can be
601 particularly valuable when coupled with GCAM and similar models to understand the
602 propagation of uncertainty in the human-Earth system [6,19,20,41].

603
604 We aim to continue the development of Matilda in a number of ways. First, we aim to develop
605 enhanced parameter sampling options to enable more robust sampling without relying heavily
606 on *a priori* assumptions about the parametric form of prior distributions. Improving this process
607 can be addressed by implementing more Bayesian approaches into parameter sampling (e.g.,
608 Markov Chain Monte Carlo sampling) [42]. Future versions of the package will also automate
609 the process of adding more parameters to a parameter set. Second, providing more methods
610 for model evaluation will improve the robustness of an analysis. While our case study assumes
611 that models can be accurately evaluated using a single scoring criterion like observed global
612 mean surface temperature, it is widely recognized that climate model evaluation is often
613 improved by considering multiple lines of evidence. Comprehensive model evaluation should

614 involve assessing performance across various observed climate variables (e.g., temperature and
615 CO₂ concentrations and the interactions among those variables) and/or existing ESMs. Finally,
616 we intend to develop further Matilda's ability to be integrated with additional RCMs. This
617 integration would provide a unified approach for conducting probabilistic projection analysis
618 across different models. By doing so, we can effectively address questions that focus on
619 clarifying uncertainties arising from structural differences among models within the RCM
620 community.
621

622 Acknowledgments

623 This research was supported by the U.S. Department of Energy, Office of Science, as part of
624 research in MultiSector Dynamics, Earth and Environmental System Modeling Program. The
625 Pacific Northwest National Laboratory is operated by Battelle for the US Department of Energy
626 (Contract No. DE-AC05-76RLO1830).
627

628 Author Contributions

629 **Conceptualization:** Joseph K. Brown, Ben Bond-Lamberty.

630 **Data curation:** Joseph K. Brown, Ben Bond-Lamberty.

631 **Methodology:** Joseph K. Brown, Ben Bond-Lamberty, Leeya Pressburger, Kalyn Dorheim, Abigail
632 Snyder, Claudia Tebaldi, Steven J. Smith.

633 **Software:** Joseph K. Brown, Ben Bond-Lamberty, Leeya Pressburger, Abigail Snyder, Claudia
634 Tebaldi.

635 **Writing – Original Draft Preparation:** Joseph K. Brown.

636 **Visualization:** Joseph K. Brown

637 **Writing – Review & Editing:** Ben Bond-Lamberty, Leeya Pressburger, Kalyn Dorheim, Abigail
638 Snyder, Claudia Tebaldi, Steven J. Smith.

639 **Project Administration:** Ben Bond-Lamberty.

640 **Supervision:** Ben Bond-Lamberty.
641

642 References

- 643 1. Moss RH, Edmonds JA, Hibbard KA, Manning MR, Rose SK, van Vuuren DP, et al. The next
644 generation of scenarios for climate change research and assessment. *Nature*. 2010
645 Feb;463(7282):747–56.
- 646 2. van Vuuren DP, Kok MTJ, Girod B, Lucas PL, de Vries B. Scenarios in Global Environmental
647 Assessments: Key characteristics and lessons for future use. *Glob Environ Change*. 2012 Oct
648 1;22(4):884–95.
- 649 3. Alizadeh O. Advances and challenges in climate modeling. *Clim Change*. 2022 Jan 31;170(1):18.
- 650 4. O’Neill BC, Kriegler E, Ebi KL, Kemp-Benedict E, Riahi K, Rothman DS, et al. The roads ahead:
651 Narratives for shared socioeconomic pathways describing world futures in the 21st century. *Glob*
652 *Environ Change*. 2017 Jan 1;42:169–80.
- 653 5. O’Neill BC, Carter TR, Ebi K, Harrison PA, Kemp-Benedict E, Kok K, et al. Achievements and needs for
654 the climate change scenario framework. *Nat Clim Chang*. 2020 Nov 25;10(12):1074–84.
- 655 6. Hartin CA, Patel P, Schwarber A, Link RP, Bond-Lamberty BP. A simple object-oriented and open-
656 source model for scientific and policy analyses of the global climate system – Hector v1.0 [Internet].
657 Vol. 8, Geoscientific Model Development. 2015. p. 939–55. Available from:
658 <http://dx.doi.org/10.5194/gmd-8-939-2015>
- 659 7. Leach NJ, Jenkins S, Nicholls Z, Smith CJ, Lynch J, Cain M, et al. FalRv2.0.0: a generalized impulse
660 response model for climate uncertainty and future scenario exploration. *Geosci Model Dev*. 2021
661 May 27;14(5):3007–36.
- 662 8. Nicholls ZRJ, Meinshausen M, Lewis J, Gieseke R, Dommenges D, Dorheim K, et al. Reduced
663 Complexity Model Intercomparison Project Phase 1: introduction and evaluation of global-mean
664 temperature response. *Geosci Model Dev*. 2020 Oct 31;13(11):5175–90.
- 665 9. Dorheim K, Link R, Hartin C, Kravitz B, Snyder A. Calibrating simple climate models to individual
666 earth system models: Lessons learned from calibrating Hector. *Earth Space Sci* [Internet]. 2020
667 Nov;7(11). Available from: <https://onlinelibrary.wiley.com/doi/10.1029/2019EA000980>
- 668 10. Meinshausen M, Raper SCB, Wigley TML. Emulating coupled atmosphere-ocean and carbon cycle
669 models with a simpler model, MAGICC6 – Part 1: Model description and calibration. *Atmos Chem*
670 *Phys*. 2011 Feb 16;11(4):1417–56.
- 671 11. Woodard, Shiklomanov, Kravitz. A permafrost implementation in the simple carbon–climate model
672 Hector v. 2.3 pf. *Geosci Model Dev* [Internet]. 2021 Jul 30; Available from:
673 <https://gmd.copernicus.org/articles/14/4751/2021/>
- 674 12. Kikstra JS, Nicholls ZRJ, Smith CJ, Lewis J, Lamboll RD, Byers E, et al. The IPCC Sixth Assessment
675 Report WGIII climate assessment of mitigation pathways: from emissions to global temperatures.
676 *Geosci Model Dev*. 2022 Dec 20;15(24):9075–109.
- 677 13. Pressburger L, Dorheim K, Keenan TF, McJeon H, Smith SJ, Bond-Lamberty B. Quantifying airborne

- 678 fraction trends and the destination of anthropogenic CO₂ by tracking carbon flows in a simple
679 climate model. *Environ Res Lett.* 2023 Apr 21;18(5):054005.
- 680 14. Smith CJ, Forster PM, Allen M, Leach N, Millar RJ, Passerello GA, et al. FAIR v1.3: a simple
681 emissions-based impulse response and carbon cycle model. *Geosci Model Dev.* 2018 Jun
682 18;11(6):2273–97.
- 683 15. Frank P. Propagation of Error and the Reliability of Global Air Temperature Projections. *Front Earth*
684 *Sci Chin [Internet].* 2019;7. Available from:
685 <https://www.frontiersin.org/articles/10.3389/feart.2019.00223>
- 686 16. Hall J, Fu G, Lawry J. Imprecise probabilities of climate change: aggregation of fuzzy scenarios and
687 model uncertainties. *Clim Change.* 2007 Apr 1;81(3):265–81.
- 688 17. Nicholls Z, Meinshausen M, Lewis J, Corradi MR, Dorheim K, Gasser T, et al. Reduced Complexity
689 Model Intercomparison Project Phase 2: Synthesizing Earth System Knowledge for Probabilistic
690 Climate Projections. *Earths Future.* 2021 Jun;9(6):e2020EF001900.
- 691 18. Rogelj J, Fransen T, den Elzen MGJ, Lamboll RD, Schumer C, Kuramochi T, et al. Credibility gap in
692 net-zero climate targets leaves world at high risk. *Science.* 2023;380(6649):1014–6.
- 693 19. Ou Y, Iyer G, Clarke L, Edmonds J, Fawcett AA, Hultman N, et al. Can updated climate pledges limit
694 warming well below 2 C. *Science.* 2021 Nov 5;374(6568):693–5.
- 695 20. Fawcett AA, Iyer GC, Clarke LE, Edmonds JA, Hultman NE, McJeon HC, et al. Can Paris pledges avert
696 severe climate change? *Science.* 2015;350(6265):1168–9.
- 697 21. Meinshausen M, Nicholls ZRJ, Lewis J, Gidden MJ, Vogel E, Freund M, et al. The shared socio-
698 economic pathway (SSP) greenhouse gas concentrations and their extensions to 2500. *Geosci*
699 *Model Dev.* 2020 Aug 13;13(8):3571–605.
- 700 22. Dorheim K, Gering S, Gieseke R, Hartin C, Pressburger L, N. A, et al. Hector V3.1.1: functionality and
701 performance of a reduced-complexity climate model. doi:10.5194/egusphere-2023-1477
- 702 23. Dorheim K, Bond-Lamberty B, Hartin C, Link R, Nicholson M, Pralit P, et al. Hector a simple carbon-
703 climate model [Internet]. 2023. Available from: <https://zenodo.org/record/821645>
- 704 24. Evanoff J, Vernon C, Waldhoff S, Snyder A, Hartin C. hectorui: A web-based interactive scenario
705 builder and visualization application for the Hector climate model. *J Open Source Softw.* 2020 Dec
706 11;5(56):2782.
- 707 25. Jonko A, Urban NM, Nadiga B. Towards Bayesian hierarchical inference of equilibrium climate
708 sensitivity from a combination of CMIP5 climate models and observational data. *Clim Change.* 2018
709 Jul 1;149(2):247–60.
- 710 26. Smith CJ, Kramer RJ, Myhre G, Alterskjær K, Collins W, Sima A, et al. Effective radiative forcing and
711 adjustments in CMIP6 models. *Atmos Chem Phys.* 2020 Aug 17;20(16):9591–618.
- 712 27. Jones C, Robertson E, Arora V, Friedlingstein P, Shevliakova E, Bopp L, et al. Twenty-first-century
713 compatible CO₂ emissions and airborne fraction simulated by CMIP5 earth system models under

- 714 four representative concentration pathways. *J Clim.* 2013;26(13):4398–413.
- 715 28. Sherwood SC, Webb MJ, Annan JD, Armour KC, Forster PM, Hargreaves JC, et al. An assessment of
716 earth's climate sensitivity using multiple lines of evidence. *Rev Geophys* [Internet]. 2020 Dec;58(4).
717 Available from: <https://onlinelibrary.wiley.com/doi/10.1029/2019RG000678>
- 718 29. Vega-Westhoff B, Sriver RL, Hartin CA, Wong TE, Keller K. Impacts of observational constraints
719 related to sea level on estimates of climate sensitivity. *Earths Future.* 2019 Jun;7(6):677–90.
- 720 30. Ito A. A historical meta-analysis of global terrestrial net primary productivity: are estimates
721 converging? *Glob Chang Biol.* 2011 Oct;17(10):3161–75.
- 722 31. Davidson EA, Janssens IA. Temperature sensitivity of soil carbon decomposition and feedbacks to
723 climate change. *Nature.* 2006 Mar;440(7081):165–73.
- 724 32. Eriksson O, Jauhiainen A, Maad Sasane S, Kramer A, Nair AG, Sartorius C, et al. Uncertainty
725 quantification, propagation and characterization by Bayesian analysis combined with global
726 sensitivity analysis applied to dynamical intracellular pathway models. *Bioinformatics.* 2018 Jul
727 13;35(2):284–92.
- 728 33. Tans P, Keeling R. Mauna Loa CO2 annual mean data. NOAA/ESRL. 2015;
- 729 34. Morice CP, Kennedy JJ, Rayner NA, Winn JP, Hogan E, Killick RE, et al. An updated assessment of
730 near-surface temperature change from 1850: The HadCRUT5 data set. *J Geophys Res* [Internet].
731 2021 Feb 16;126(3). Available from: <https://onlinelibrary.wiley.com/doi/10.1029/2019JD032361>
- 732 35. Massoud EC, Lee H, Gibson PB, Loikith P, Waliser DE. Bayesian Model Averaging of Climate Model
733 Projections Constrained by Precipitation Observations over the Contiguous United States. *J*
734 *Hydrometeorol.* 2020 Oct 1;21(10):2401–18.
- 735 36. Vrugt JA, Massoud EC. Uncertainty quantification of complex system models: Bayesian analysis.
736 *Handbook of hydrometeorological ensemble* [Internet]. 2019; Available from:
737 https://scholar.google.ca/scholar?cluster=14238340407635547794&hl=en&as_sdt=0,5&scioldt=0,5
- 738 37. Khan F, Pilz J, Ali S. Evaluation of CMIP5 models and ensemble climate projections using a Bayesian
739 approach: a case study of the Upper Indus Basin, Pakistan. *Environ Ecol Stat.* 2021 Jun 1;28(2):383–
740 404.
- 741 38. Hodson TO. Root-mean-square error (RMSE) or mean absolute error (MAE): when to use them or
742 not. *Geosci Model Dev.* 2022 Jul 19;15(14):5481–7.
- 743 39. Chai T, Draxler RR. Root mean square error (RMSE) or mean absolute error (MAE)? – Arguments
744 against avoiding RMSE in the literature. *Geosci Model Dev.* 2014 Jun 30;7(3):1247–50.
- 745 40. Intergovernmental Panel on Climate Change (IPCC). Future Global Climate: Scenario-based
746 Projections and Near-term Information. In: *Climate Change 2021 – The Physical Science Basis:*
747 *Working Group I Contribution to the Sixth Assessment Report of the Intergovernmental Panel on*
748 *Climate Change.* Cambridge University Press; 2023. p. 553–672.
- 749 41. Riahi K, Grübler A, Nakicenovic N. Scenarios of long-term socio-economic and environmental

- 750 development under climate stabilization. *Technol Forecast Soc Change*. 2007 Sep 1;74(7):887–935.
- 751 42. Tsutsui J. Minimal CMIP Emulator (MCE v1. 2): a new simplified method for probabilistic climate
752 projections. *Geoscientific Model Development*. 2022;15(3):951–70.

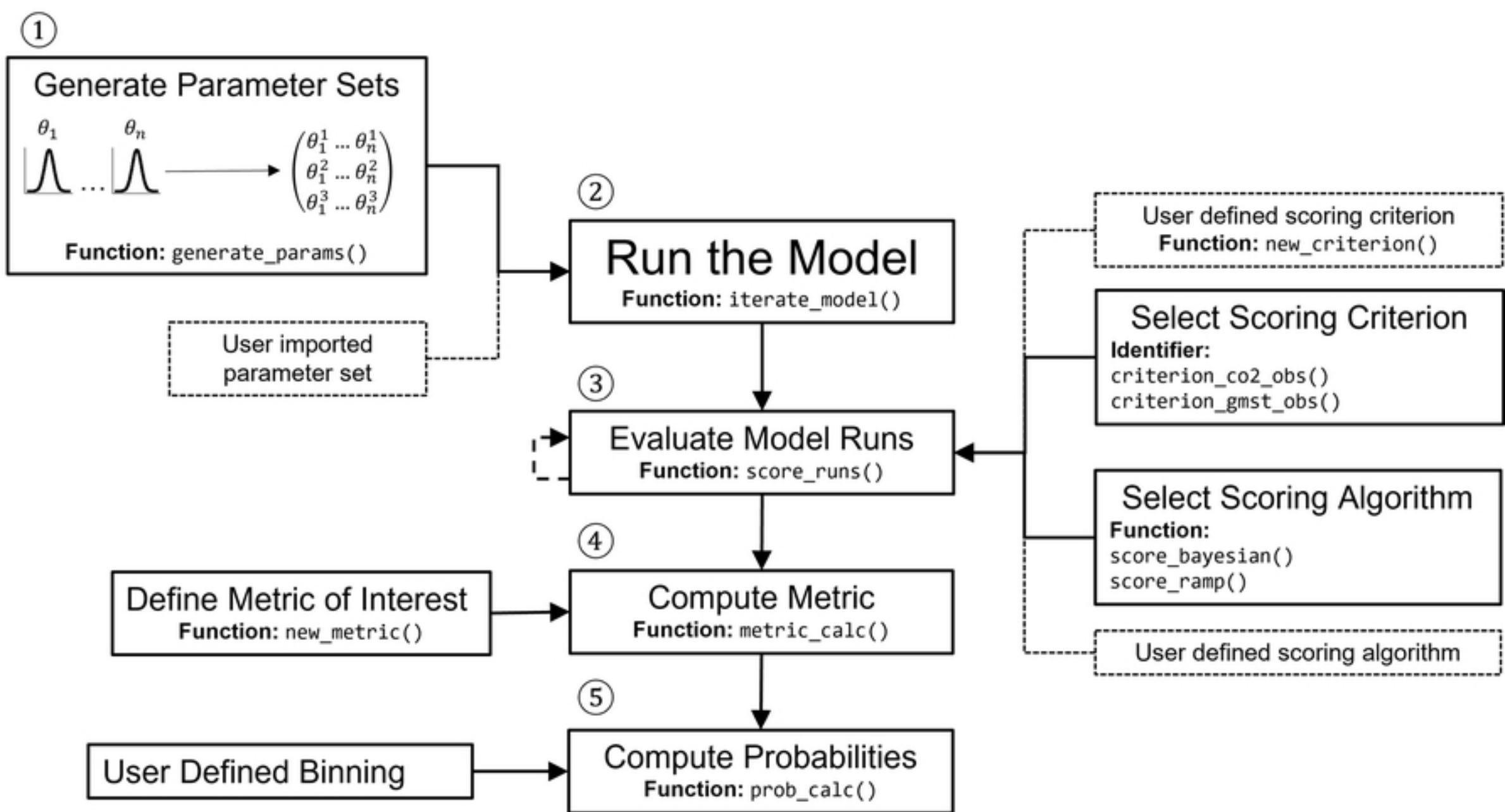


figure_01

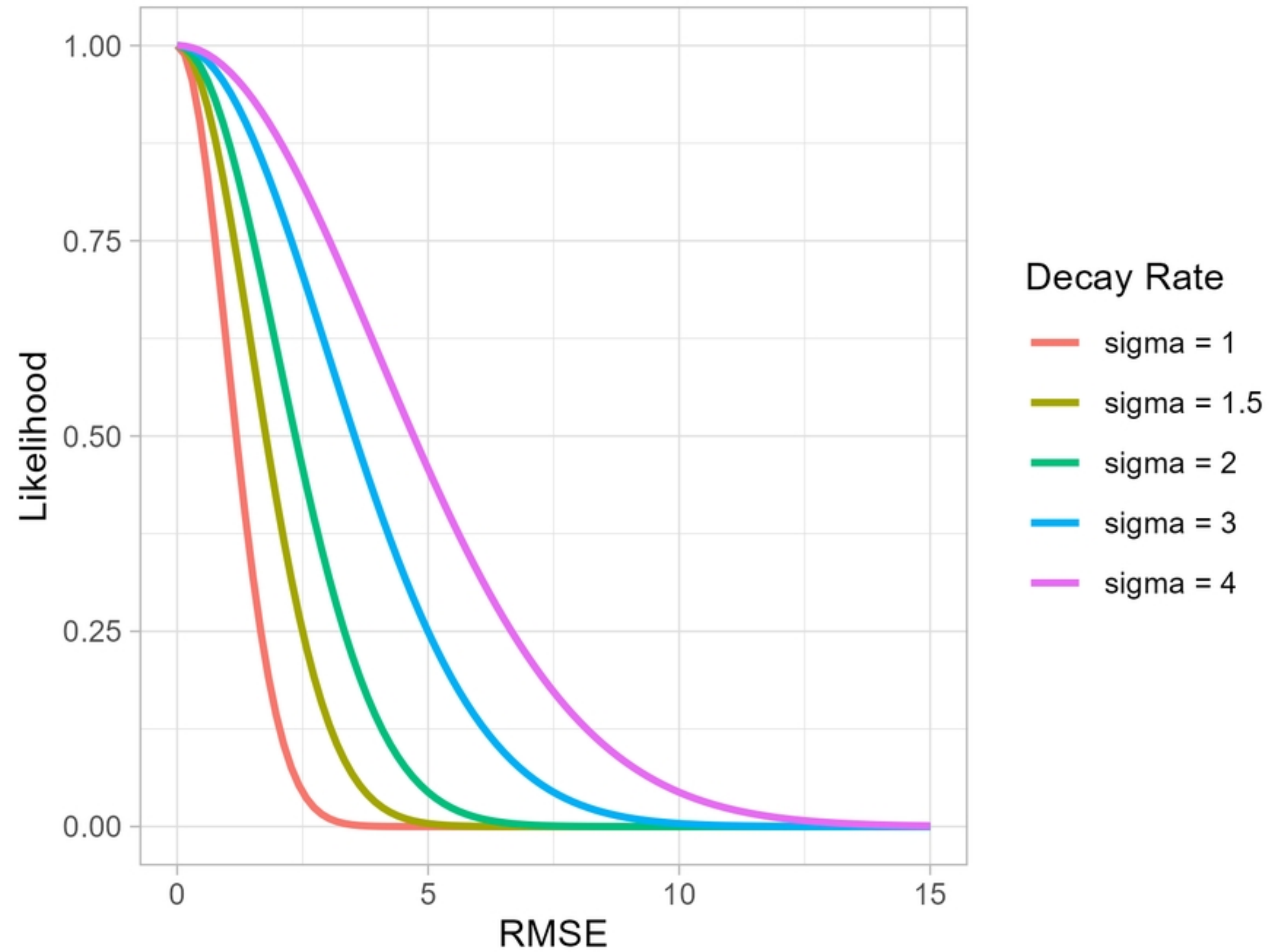


figure_02

This manuscript is a preprint and has not been peer reviewed. The copyright holder has made the manuscript available under a [Creative Commons Attribution 4.0 International \(CC BY\) license](#) and consented to have it forwarded to [EarthArXiv](#) for public posting.

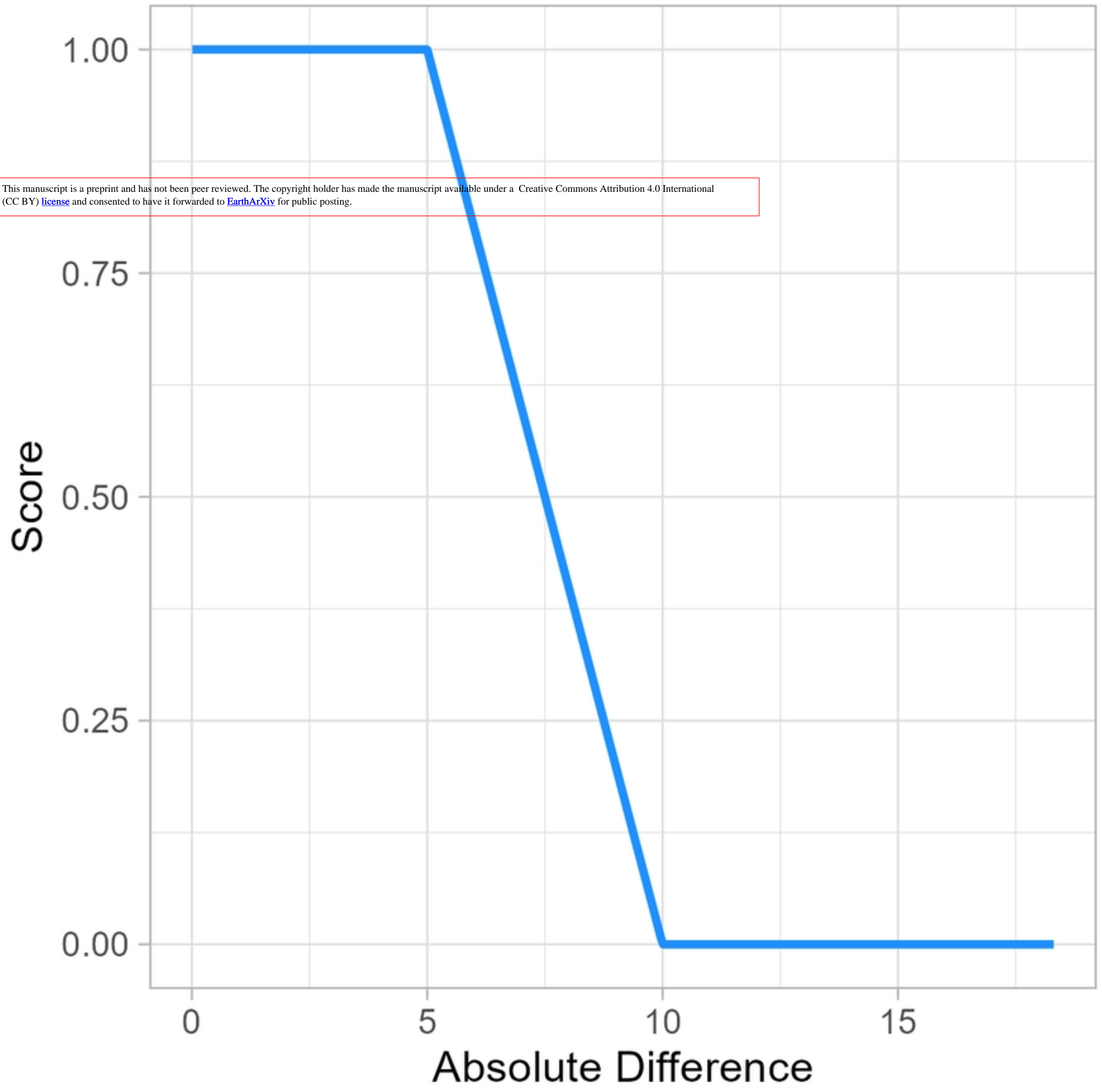
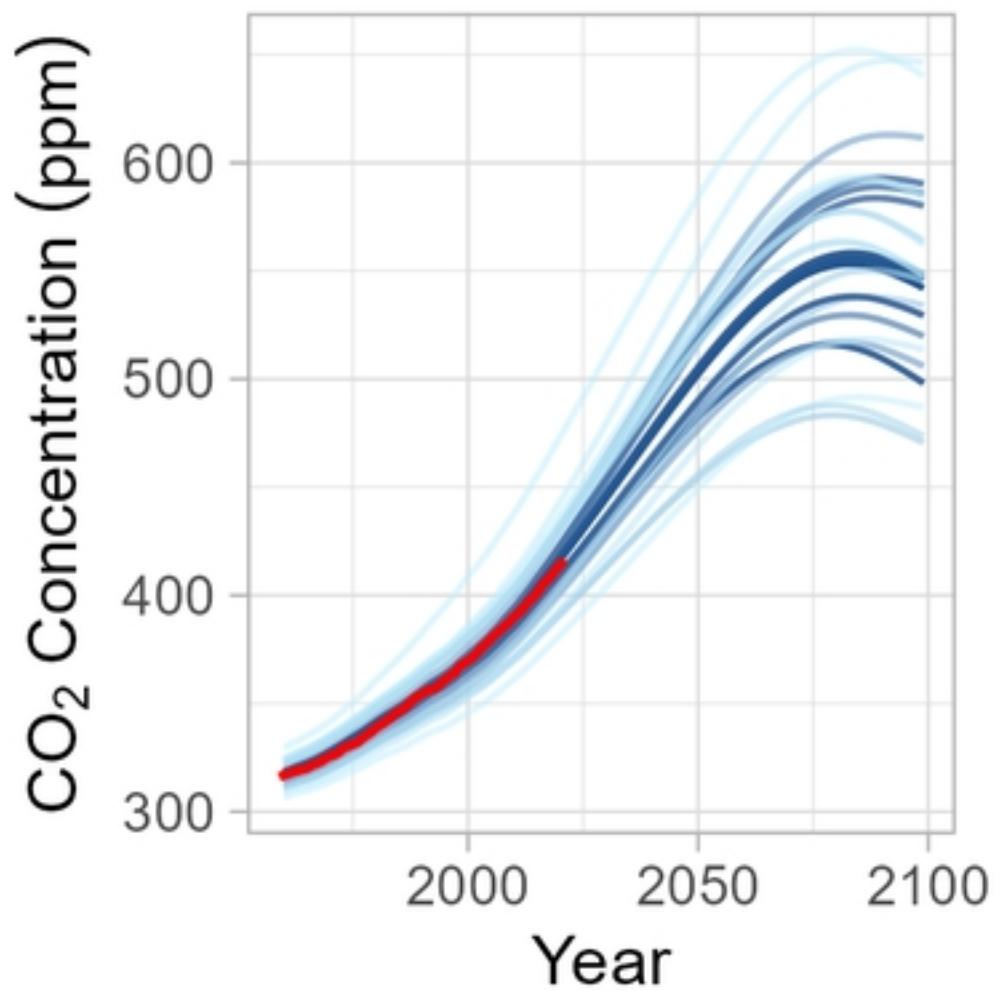


figure_03

A) score_ramp()



B) score_bayesian()

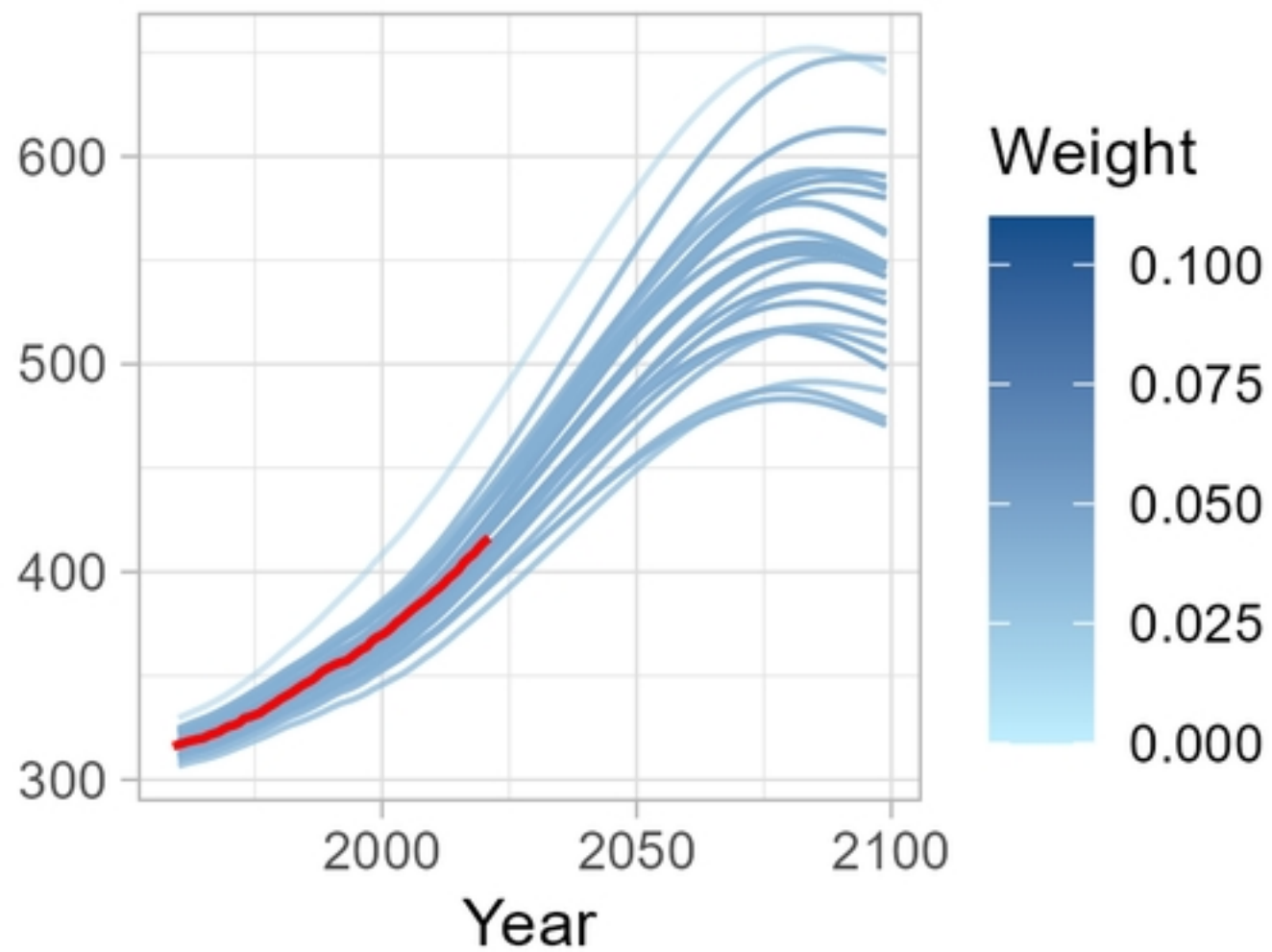


figure_04

This manuscript is a preprint and has not been peer reviewed. The copyright holder has granted EarthArXiv a Creative Commons Attribution 4.0 International (CC BY) license and consented to have it forwarded to EarthArXiv for public posting.

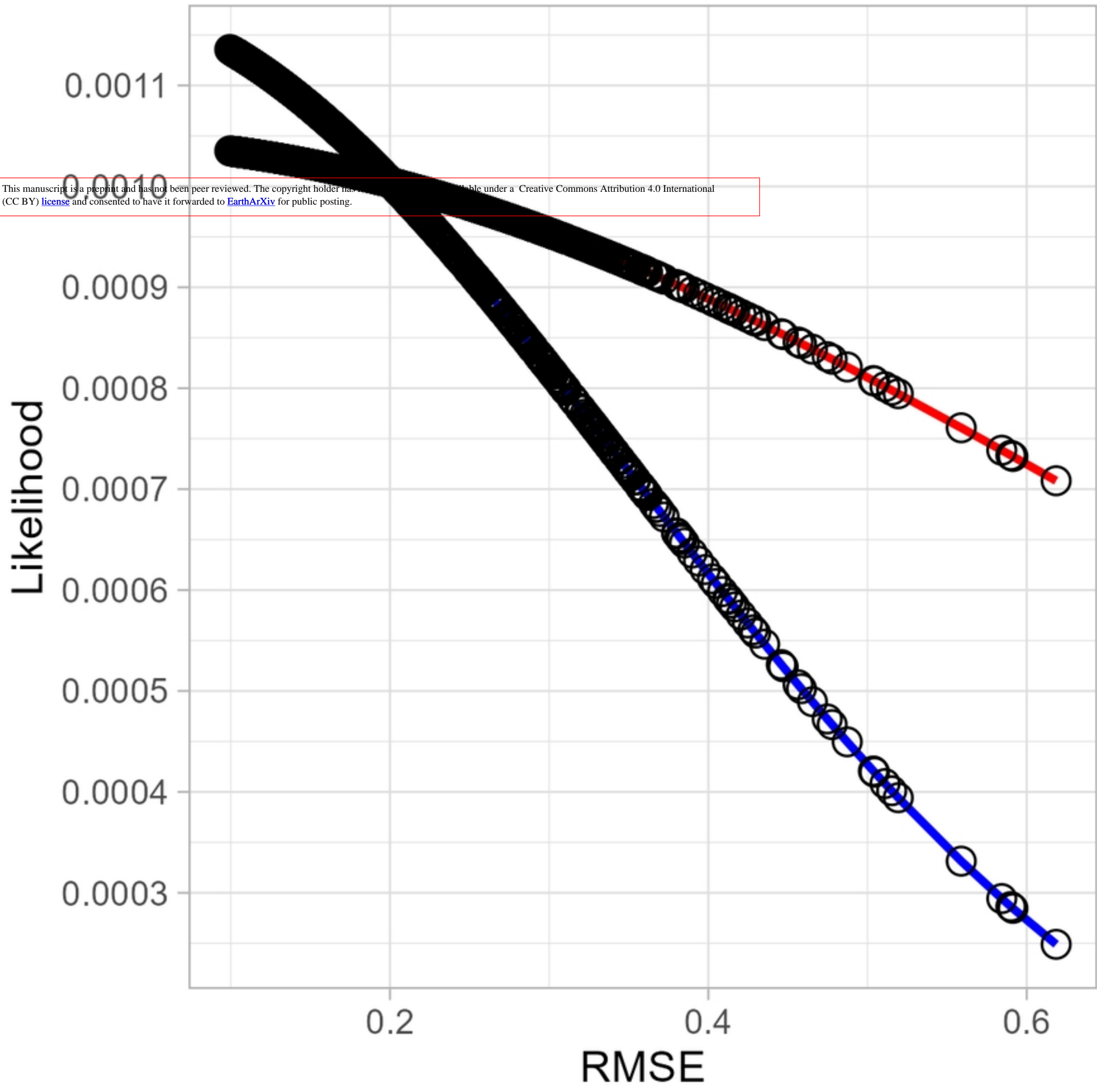
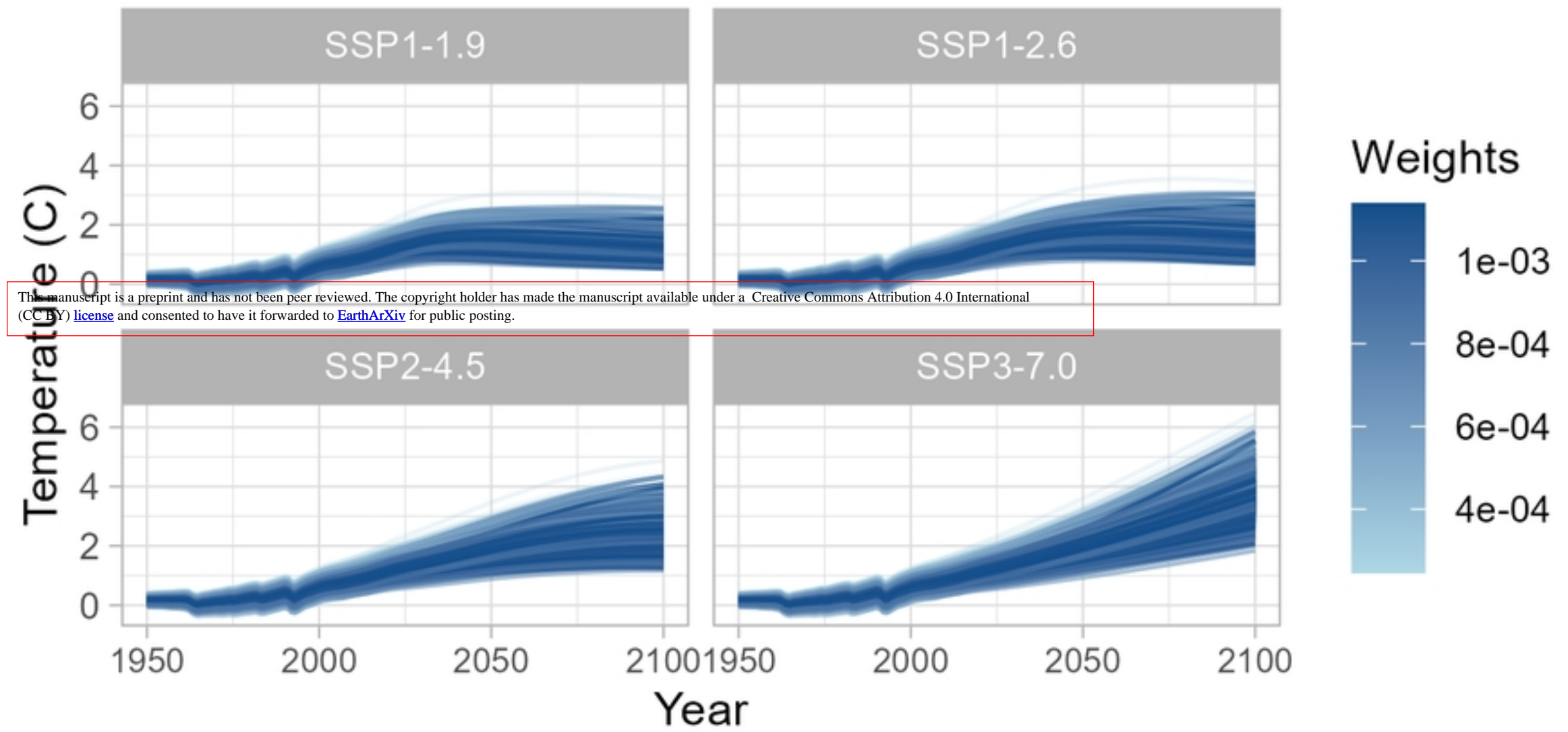


figure_05

A)



B)

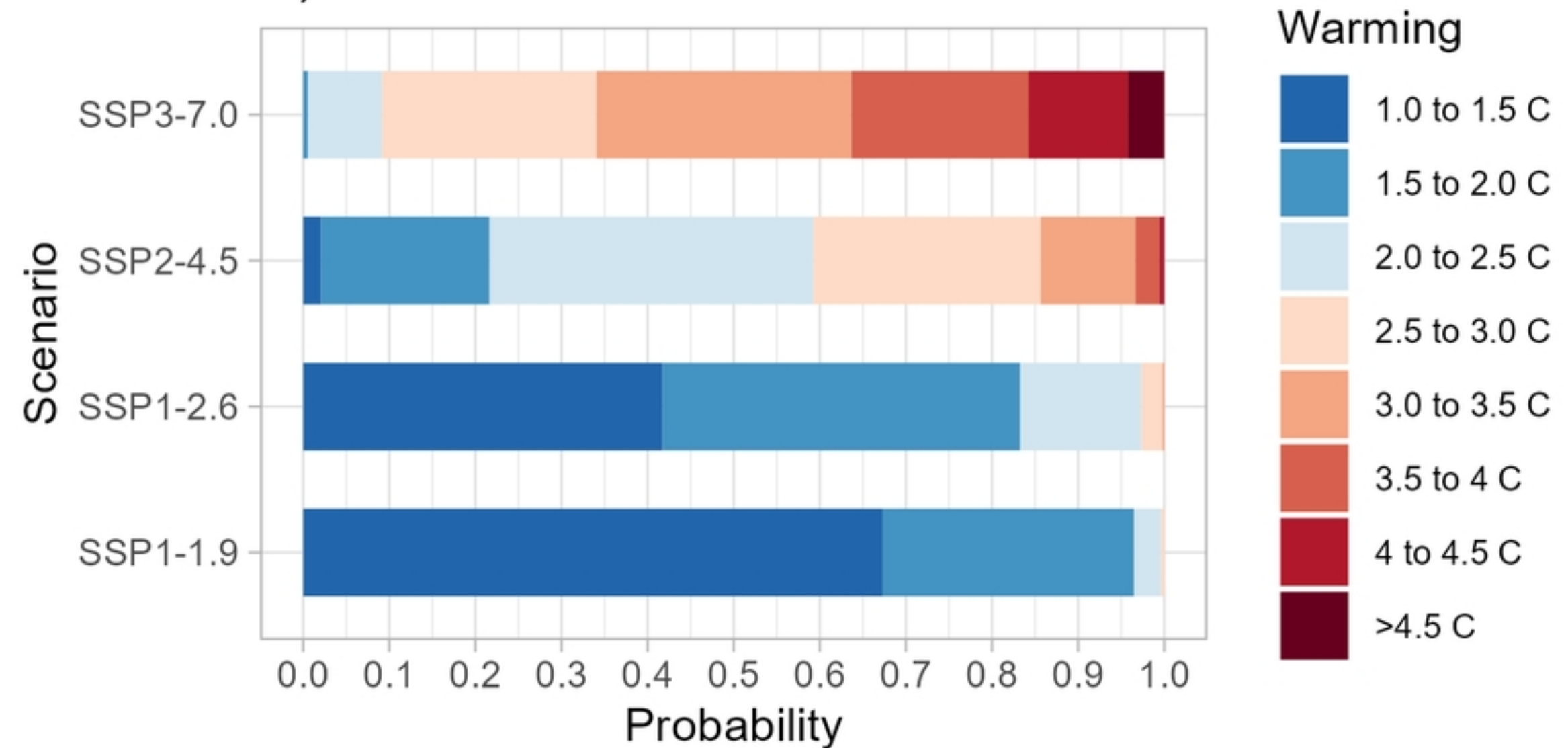


figure_06